J Mater Sci (2008) 43:4399–4410
DOI 10.1007/s10853-008-2595-0

Damage evolution and energy absorption of E-glass/polypropylene laminates subjected to ballistic impact

L. J. Deka · S. D. Bartus · U. K. Vaidya

Received: 4 November 2007 / Accepted: 13 March 2008 / Published online: 18 April 2008

Abstract High-velocity transverse impact of laminated fiber reinforced composites is of interest in military, marine and structural applications. The overall objective of this work was to investigate the behavior of laminated thermoplastic composites of varying thicknesses under high-velocity impact from an experimental and modeling viewpoint. In order to analyze this problem, a series of ballistic impact tests have been performed on plain weave E-glass/polypropylene (E-glass/PP) composites of different thicknesses using 0.30 and 0.50 caliber right-cylinder shaped projectiles. A gas gun with a sabot stripper mechanism was employed to impact the panels. In order to analyze the perforation mechanisms, ballistic limit and damage evaluation, an explicit three-dimensional finite element code LS-DYNA was used. Material model 162, a progressive failure model based on modified Hashin's criteria, has been assigned to analyze failure of the laminate. The projectile was modeled using Material model 3 (MAT_PLASTIC_KINEMATIC). The laminates and the projectile were meshed using brick elements with single integration points. The impact velocity ranged from 187 to 332 m s^{-1}. Good agreement between the numerical and experimental results was attained in terms of predicting ballistic limit, delamination and energy absorption of E-glass/PP laminate.

L. J. Deka · U. K. Vaidya (✉)
Department of Material Science & Engineering, The University of Alabama at Birmingham, Birmingham, AL 35294-4461, USA
e-mail: uvaidya@uab.edu

S. D. Bartus
Army Research Laboratory, Aberdeen, MD, USA

Introduction

Polymer matrix composite materials have realized steady increase in the number of applications in military vehicles, marine vessels and aerospace structures [1]. The structures are oftentimes subjected to damage from high-velocity projectiles and small fire arms. In a composite laminate subjected to ballistic impact, the kinetic energy of the projectile is dissipated through several mechanisms. The predominant energy absorption mechanisms are as follows: kinetic energy imparted to the specimen, namely cone formation on the distal side of the laminate and/or spall formation, energy absorption as a result of shear plugging, tensile fiber failure of the primary yarns, fiber debonding, fiber pull-out, elastic deformation of the secondary yarns, matrix cracking, interlaminar delamination, and frictional energy absorbed during interaction of the penetrator and laminate [2–5].

Over the last several decade, a significant body of work has focused on experimental and theoretical research on the transverse impact response of polymer matrix composite laminates in order to gain insight into failure mechanisms and energy absorption. Most of the work to date has focused on thermoset composites [6–9] or high-performance thermoplastic composites [10]. The focus of this work is to evaluate the response of thermoplastic composite materials under high-velocity impact with the aid of experiments and finite element modeling.

Wen [11, 12] investigated the perforation and penetration of fiber reinforced plastic (FRP) laminates using different projectile shapes, e.g. semi-hemispherical, conical, ogive, and flat. In this work, Wen proposed analytical equations based on material properties and the static punch curve for various projectile geometries in order to predict the ballistic limit. Lee and Sun [7] experimentally evaluated

the dynamic penetration of Carbon Fiber Reinforced Plastic (CFRP) laminates for a velocity range of 21- 91 m s^{-1} for a flat-end cylindrical projectile. They defined the penetration process in three distinct stages: pre-delamination (fiber crushing), post-delamination before plugging, and post-plugging. Mines et al. [6] studied transverse impact of E-glass/polyester laminates of different thicknesses with different projectile shapes. They found that the energy absorption mechanisms during penetration and perforation also exhibited the same behavior noted by Lee and Sun [7].

A significant amount of work has focused on modeling failure mechanisms of laminated polymer matrix composites subjected to transverse impact loading [13–19]. However, it is generally agreed that composites fail in a progressive manner. Ladeveze et al. [20, 21] used damage mechanics approach to describe matrix cracking and fiber/matrix debonding by introducing damage variables associated with material stiffness reduction in their plasticity model. Johnson et al. [22] reported a numerical method to predict composite damage using Continuum Damage Mechanics (CDM) using the framework outlined by Ladeveze et al. [20, 21]. Matzenmiller et al. [23] developed a CDM model for unidirectional composites. On the basis of CDM, Williams and Vaziri [24] wrote material subroutines for matrix/fiber failure in LS-DYNA [24]. Yen [25] developed Material Model 161 and 162 (MAT 161/162) for LS-DYNA that captures the progressive failure mode of composite laminates of both unidirectional and plain weave construction, subjected to transverse impact. Because of the inherent ability to model progressive damage MAT 161/162 has been used successfully in predicting energy absorption and damage [25–28]. The objective of the current study was to model energy absorption and damage evolution in plain-weave thermoplastic composite laminates subjected to transverse high-velocity impact at or near ballistic limit, V_B.

Experimental procedure

E-glass (Owens Corning 225 4588) and Polypropylene (PP) (BP Amoco 9965) were used to produce 12 mm wide tapes with an average thickness of 0.60 mm using a hot-melt impregnation process. The tapes were subsequently woven into plain weave fabric architecture preform and consolidated into 8, 12, and 16-layer laminates using a 30 × 30 cm^2 mold. This corresponded to average thickness of 5.25, 8.15, and 11.00 mm for the 8, 12, and 16-layer laminates, respectively. The consolidated material had an average fiber content of 67% weight (42% volume) and density 1,585 kg m^{-3}.

A single-stage light gas gun consisting of a pressure chamber, a barrel and a nitrogen/helium tank was used to launch the projectiles. The impactors were 0.30 caliber (7.90 mm) and 0.50 caliber (12.7 mm) right cylinders made of alloyed tool steel with a mass of 2.67 g ± 0.05 g (0.30 caliber) and 13.40 g ± 0.03 g (0.50 caliber), which is consistent with the mass of the corresponding NATO Fragment Simulating Projectiles (FSP) [29]. The projectile velocity was measured using photoelectric chronographs (Model: Oehler 35 and Oehler Sky Screens). The impact velocity was decreased from the full penetration condition to ballistic limit, V_B or partial penetration condition in accordance with the V_{50} definition for the 8, 12, and 16 layer laminates. Four to five specimens were tested for each laminate thickness. Ballistic limit, V_B refers to the minimum velocity at which a projectile consistently and completely penetrates the target of given thickness and physical properties at a specified angle of obliquity, whereas V_{50} is the velocity at which penetration is likely to occur for 50% of the impacts [5].

Numerical approach

Simulation tools

Altair Hypermesh v7.0 [30] and Finite Element Model Builder (eta/FEMB-PC v28.0) [31] were used in pre-processing. LS-DYNA (v970) [32] was used to analyze perforation mechanisms, failure modes, and damage evaluation during high-velocity projectile impact of the E-glass/PP composite plates described in the previous section.

Numerical model creation

The composite plate and the projectile were meshed in Hypermesh^{TM} using brick elements with single integration point (ELFORM = 1). The one point element is more robust than the fully integrated element (Type 2, 3) in the case of large deformation. The dimension of the target was 15 × 15 cm^2 and number of layers used in each plate determined the target thickness of 8, 12, and 16 layer laminates. Each E-glass/PP laminate had 1,056 brick elements and was represented by a single element through-the-thickness, e.g. 8, 12, and 16 elements for the 8, 12, and 16 layer laminates, respectively. The right cylinder projectile was meshed with 2,800 brick elements and assigned an initial velocity which mirrored experimental conditions. The modeled geometry and initial grid are shown in Fig. 1. A fine grid, relative to the plate boundaries (brick element dimension (mm), 0.529 × 0.629 × 0.68) was used in the impact region of the target to obtain a smooth stress gradient. The mesh size increased gradually toward the outer edges, approximately up to 3.64 × 2.32 × 0.68 (mm) to

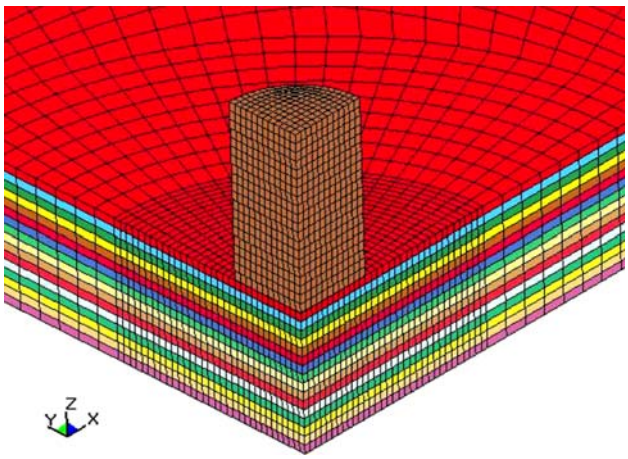

Fig. 1 Quarter symmetry geometry of the projectile and 16 layer laminate showing the mesh refinement along the periphery of the laminate

maximize computational efficiency. A coarser grid toward the edges leads to the failure of the aspect ratio (>5). Failure of aspect ratio did not affect the numerical results because the impact region and its surroundings were discretised with very fine uniform brick elements. The interaction between the projectile and composite laminate was handled with erosion logic, using a gap size 0.01 mm. A quarter symmetry approach was adopted for all the impact simulations to reduce computational time. The material properties for the composite plate and the projectile used in the simulation are shown in Tables 1–3 provides the model dimensions.

Material model

Material model 162 (MAT_COMPOSITE_DMG_MSC) captures progressive damage under high strain rate and high pressure loading was chosen to simulate the impact condition. MAT 162 is based on the Hashin's failure criteria [33], which considers five failure modes; tensile and compressive fiber failure, fiber crush, through-the-thickness matrix failure and delamination [34]. During impact simulation, some elements in the impact region undergo large distortions, which may lead to numerical instabilities; hence an element erosion criterion is incorporated in Material model 162.

A cylindrical steel projectile was modeled using Material model 3 (MAT_PLASTIC_KINEMATIC) [34]. MAT 3 is a bi-linear elastic-plastic model that contains formulations combining isotropic and kinematic hardening. In the present analysis, the hardening parameter, β was considered zero (kinematic hardening). In kinematic hardening the radius of the yield surface is fixed but the center translates in the direction of the plastic strain. There are several material models available in LS-DYNA to

Table 1 Material properties of a plain-woven PP/E-glass composite layer

Density (kg m^{-3})	ρ	1500
Young's modulus (GPa)	E_{11}	14
	E_{22}	14
	E_{33}	5.3
Shear modulus	G_{21}	1.79
	G_{31}	1.52
	G_{32}	1.52
Possions's ratio	V_{21}	0.08
	V_{31}	0.14
	V_{32}	0.15
Tensile strength (GPa)	X_T	0.43
	Y_T	0.43
	Z_T	0.15
Compressive strength (GPa)	X_C	0.23
	Y_C	0.23
Matrix mode shear strength (Gpa)	S_{12}	0.032
	S_{23}	0.032
	S_{31}	0.03
Fiber shear strength (GPa)	S_{FS}	0.25
Fiber crush strength (GPa)	S_{FC}	0.65
E_limit		2
Delamination factor	S	0.3
Friction angle	Φ	20
Strength properties strain rate coefficient	C_1	0.024
Longitudinal modulii strain rate coefficient	C_2	0.0066
Shear modulii strain rate coefficient	C_3	−0.07
Transverse Modulii strain rate coefficient	C_4	0.0066

Table 2 Material properties for the tool steel projectile

Density (kg m^{-3})	ρ	7860
Young's modulus (GPa)	E	210
Poisson's ratio	v	0.28
Yield strength (GPa)	σ_y	1.08

Table 3 Dimensions of quarter symmetry model

1/4 plate		
Length (mm)	50	
Width (mm)	50	
Layer thickness (mm)	0.68	
	0.30 caliber	0.50 caliber
1/4 projectile		
Radius (mm)	3.98	6.35
Length (mm)	6.96	13.65

represent the deformation behavior of steel at high strain rate and temperature conditions. In the experimental study negligible amount of deformation of the impacted face of the cylindrical projectile was observed. The other option for modeling a non-deformable projectile is Material model 20 (MAT_RIGID). MAT 20 was not considered in the present study because it does not compute stress-strain behavior of the projectile. However, MAT 3 is computationally cost-effective and used for solid elements.

Sun et al. [3] investigated the quasi-static indentation and dynamic response of graphite epoxy laminates. They concluded that given the failure modes under impacts exceeding perforation and those obtained from static punch through tests can be used in a dynamic model to predict high-speed impact and penetration. In a similar study, Xiao et al. [28] investigated the failure modes in S2-glass/SC-15 epoxy laminates under quasi-static punch shear test from experimental and numerical analysis. They reported reasonable agreement between experimental and simulations in terms of load–displacement curves, damage sequence, and damage size. Since the damage mechanisms in high-velocity impact are similar to those in quasi-static loading, the strength properties of the E-glass/PP laminate in the present study were taken from quasi-static tests. Material properties relating to the strain rate sensitivity and erosion were taken from [27]. The fiber mode crush strength (SFC) and shear strength (SFS) strongly affect the ballistic limit. These two values were found to have a strong influence in terms of obtaining correlations with experimental results. Xiao et al. [28] reported in their study that SFC and SFS of E-glass were measured as 607–758 and 228–310 MPa, respectively.

Energy and model sensitivity

During high-velocity impact, the kinetic energy of the projectile is transferred to the plate and absorbed through the various damage mechanisms, thereby increasing the internal energy of the system. LS-DYNA verifies the simulation by conservation of energy of the system. The energy transferred to the composite plate from the projectile can be expressed by:

$$E_{\text{tran}} = \text{IE}_{\text{plate}} + \text{KE}_{\text{plate}} + \text{HGE}_{\text{plate}} + \text{KE}^{\text{erode}} + \text{IE}^{\text{erode}} + |\text{SLE}| \quad (1)$$

In the dynamic simulation, hour glass energy (HE) modes represent non-physical, zero-energy modes of deformation that produce zero strain and stress. An accurate simulation requires very small Hour Glass Energy (HGE) (<10% of the peak of the internal energy (IE)) and positive sliding energy (SLE) which determines perfect global energy balance. The global energy balance of a representative 12-layer composite plate at incident velocity of 330.4 m s^{-1} is shown in Fig. 2a. Negligible amount of HGE (curve C) is observed. High amount of HGE leads to modeling instability. Mesh refinement and proper selection of the HGE coefficient reduced hour glassing in the model. In this work, Hourglass (HG) type 4 (QM = 0.1) was used. Hourglass type 4 provides a stiffness-based control, thereby minimizing distortion of the elements, hence it is effective in inhibition of HG modes in structural parts. KE^{erode} and IE^{erode} in Eq. 1 represent kinetic energy and internal energy associated with the eroded elements.

Contact type

Proper contact definition between projectile and the laminate is required to model high-velocity transverse impact. Three different types of contacts are adopted between the impactor (slave) and the target (master) in LS-DYNA, namely: kinematic constraint method, the penalty method and the distributed parameter method. Soft constraint formulation and segment-based penalty contact (CONTACT_ERODING_SINGLE_SURFACE) were considered in this work to establish contact between the projectile and the composite plate. In the soft constraint option (SOFT = 1), nodal mass and time step determine the contact stiffness at the interface where two nodal masses are separated by a spring. Negative contact energy is sometimes generated when parts slide relative to one another. This effect was minimized by controlling the initial node penetration and time step scale factor as shown in Fig. 2a. Segment-based contact algorithm (SOFT = 2)

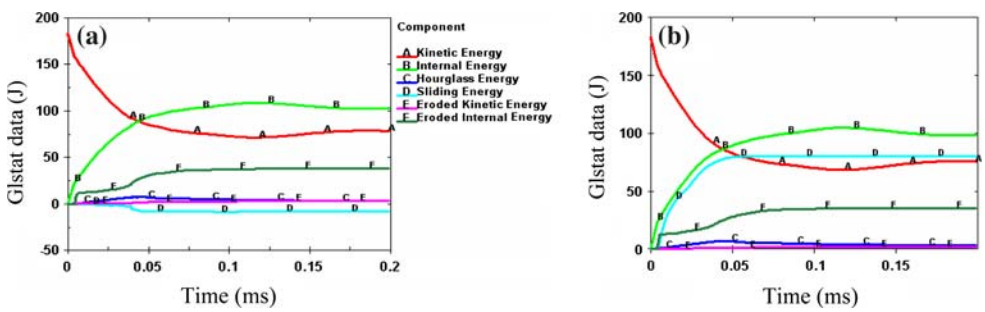

Fig. 2 Global energy balance of 12 layer composite laminate with (**a**) soft constrain formulation, SOFT = 1 and (**b**) segment-based penalty contact, SOFT = 2

checks segment versus segment penetration and does not use the shooting node logic parameter because it ignores the initial penetration due to the symmetry of the approach as illustrated in Fig. 2b.

The SOFT = 2 option resulted in very high positive sliding energy (>10% of total energy) as shown in Fig. 2b. Soft constraint option (SOFT = 1) was adopted in all the simulations ignoring the small negative energy effect. High-velocity impact tests generate high pressure at the contact interfaces and sometimes unacceptable penetration may occur. This can be avoided by scaling up the stiffness (SOFSCL) or scaling down the time step size [34]. In high-velocity impact modeling, the effect of frictional forces in interfaces is typically assumed negligible. The static friction (FS) is greater than the dynamic friction (FD); in this work FD was considered to be 0.1 and 0.3 for FS.

Progressive damage and damage parameters

A CDM formulation was incorporated in MAT 162 by adopting the MLT damage mechanics approach, Matzenmiller et al. [23], hence post-failure mechanisms in composite plates are characterized by a reduction in material stiffness. The stiffness reduction (elastic modulus) can be expressed in terms of associated damage parameters ϖ_i, given by [34]:

$$E_{\text{red}} = (1 - \varpi_i)E_i \tag{2}$$

Damage variables, grow according to Eq. 3 [34]:

$$\varpi_i = 1 - e^{\frac{1}{m_i}\left(1 - r_i^{m_i}\right)}, \quad i = 1, \ldots, 6 \tag{3}$$

where ϖ_i = damage variable, m_i = strain softening parameter (also known as damage parameter) and r_i = damage threshold. The damage variable ϖ_i varies from 0 to 1.0 as r_i varies from 1 to ∞, respectively. here are four strain softening input parameters (m_1-fiber damage in x direction, m_2-fiber damage in y direction, m_3-fiber crush and punch shear damage, and m_4-delamination damage) used in MAT 162. These damage parameters provide the softening response in the post-failure regime of the stress-strain curve. In order to understand the effect of the softening parameter 'm'on the damage progression, a single brick element with dimensions 0.5 × 0.5 × 0.5 mm^3 was loaded in uniaxial tension. The effect of the exponent m on the stress-strain response of the element is shown in Fig. 3.

High values of m (i.e. m = 50) result in brittle failure of the material. Once the tensile stress reaches the maximum value, it becomes zero which means there is no loss in stiffness prior to failure. Low values of m clearly indicate a ductile failure response resulting in more energy absorption prior to complete damage with a gradual loss of stiffness after failure. In the present study, it was found that higher values of m underpredict energy absorption of the plate,

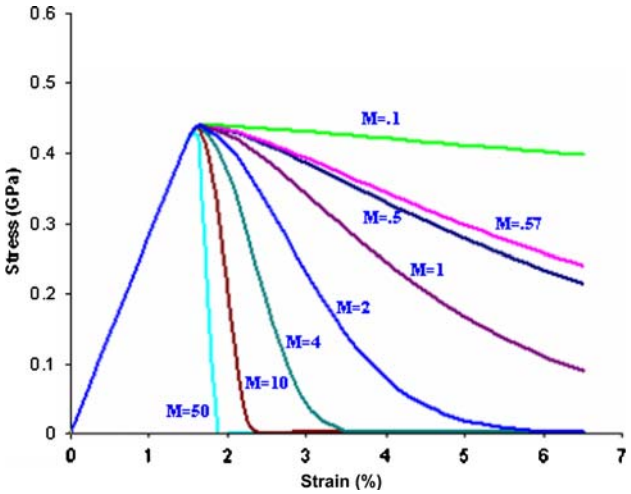

Fig. 3 Stress–strain response of the single element loaded in-plane tension with different values of m parameter

while lower values of m over predict energy absorption as illustrated in Fig. 3. Brown et al. [27] and Xiao et al. [28] conducted a sensitivity study of all four damage parameters for plain weave S-2 glass/SC-15 epoxy and E-glass/PP composites under quasi-static loading. They considered different m values corresponding to the different damage modes. It is established that the failure mechanisms involved in quasi-static punch shear test and high-velocity impact on composites are similar, while the extent of damage and time-scale of occurrence are different [3].

Results and discussion

Impact experiments

Ballistic impact tests were performed on 8, 12, and 16-layer E-glass/PP composite laminates. Four or five samples of each thickness were impacted by either a 0.30 caliber or 0.50 caliber flat-end cylinder with average projectile mass of 2.67 g ± 0.05 g and 13.40 g ± 0.01g, respectively, for these calibers. Initially all the samples were impacted above the ballistic regime, and subsequently the impact velocity was reduced to achieve the ballistic limit. For the 0.30 caliber impacts, only the 8-layer laminate was considered, since penetration was not achieved for the 12 and 16 layer laminate for the velocity range (150–250 m s^{-1}) of the tests. Table 4 provides the impact results for the 0.30 caliber projectile impact on 8-layer laminates. The table summarizes the incident and residual velocity, energy absorbed, and the parameters used for the numerical simulations. In addition to 8 layer, the 12 and 16 layer laminates were impacted with a 0.50 caliber projectile. Table 5 summarizes the 0.50 caliber results for different laminate thickness; i.e. 8, 12 and 16 layers.

Table 4 Experimental result of 0.30 caliber impact on 8 layer plates and effect of the m parameter on energy absorption of the plate

Specimen	Projectile	Projectile mass (g)	Incident velocity (m s^{-1})	Incident kinetic energy (J)	Residual velocity (m s^{-1})	Residual kinetic energy (J)	Energy absorbed (J)	Average energy absorbed (J)	Damage parameter, m_i	Numerical prediction of energy absorbtion (J)
1 (8 layers)	0.30 caliber	2.66	356	168.6	192.3	49.2	119.4		0.1	177.34
2 (8 layers)	0.30 caliber	2.82	264	98.2	0	0	98.2	130.1	0.57	125.49
3 (8 layers)	0.30 caliber	2.817	328.6	152.1	104.5	15.4	136.7		4	104
4 (8 layers)	0.30 caliber	2.66	370	182.1	189.6	47.8	134.3		50	81.52

Impact simulations and comparison to experiments

0.30 caliber impact

The initial velocities used for the simulation were identical to those used in the experimental tests. The effect of different m parameters on energy absorption during high-velocity impact of an 8 layer E-glass/PP laminate by a 0.30 cal. right cylinder steel projectile are shown in Table 4. In the case of the 0.30 caliber projectile, only 8-layer laminates were impacted. Penetration was not achieved for the 12- and 16-layer laminates using the 0.30 caliber projectile for the velocity range 150–250 m s^{-1}; hence this study was limited to 8-layer laminates only. For the sake of simplicity, the softening parameter m was assumed to be identical ($m = 0.57$) for the four strain softening damage modes. The softening parameter m was varied until the energy absorption and damage matched the experimental results. With the softening parameter, $m = 0.57$, energy absorption predicted by the model was within 96.5% of the 0.30 caliber experimental impact data, and progressive failure of the plate was adequately captured. The value of $m = 0.57$ was used as a basis in the modeling of the 0.50 caliber impacts for the 8, 12, and 16 layer laminates.

0.50 caliber impact

Table 5 shows the approximate V_{50} values for the 8, 12, and 16 layer plates impacted by the 0.50 caliber projectile. The velocities were 181.3, 272.5, and 288.8 m s^{-1}, which corresponded to impact energy absorption of 220.2, 497.5, 558.8 J for the 8, 12, and 16 layer laminates, respectively. Figure 4 illustrates that the kinetic energy dissipated by the projectiles obtained from simulations with input damage parameter, $m = 0.57$ are 220.2, 311.3, and 463.9 J, which is 100, 62.5, and 83% of the corresponding experimental results. The kinetic energy of the projectile was reduced to zero in the 8 layer laminate simulation, which was the experimental ballistic limit indicating that the damage parameter, $m = 0.57$ provides excellent correlation between the numerical and experimental data.

Figure 4 compares ballistic limit velocities obtained from simulations with those determined experimentally. With a damage parameter, $m = 0.57$, the ballistic limits predicted for the 8, 12 and 16 layers plates were 181.3, 230.0, and 265.0 m s^{-1}, respectively. This corresponded to 100, 84, and 92% agreement with the experimental results for the 8, 12, and 16 layer laminates, respectively. Using a softening parameter of $m = 0.57$, 0.325, and 0.42 for the 8, 12, and 16 layer laminates, respectively, yielded 100% agreement with the experimental results. A discussion is provided later in this section.

Table 5 Experimental impact result and numerical prediction for 0.50 caliber impact on the 8, 12, and 16 layer E-glass/PP plates

Specimen	Incident velocity energy ($m\ s^{-1}$)	Incident kinetic energy (J)	Residual velocity ($m\ s^{-1}$)	Residual kinetic energy (J)	Energy absorbed (J)	Mean experimental ballistic limit ($m\ s^{-1}$)	Standard deviation for ballistic limit ($m\ s^{-1}$)	Numerical prediction of ballistic limit ($m\ s^{-1}$)
1 (8 layers)	237.1	376.2	NR	NR	376.2	181.3	18.7	179.5
2 (8 layers)	226.2	342.2	NR	NR	342.2			
3 (8 layers)	207.9	289.1	NR	NR	289.1			
4 (8 layers)	187.1	234.3	63.7	27.1	207.2			
5 (8 layers)	186.8	233.5	0.0[a]	0.0[a]	233.5			
1 (12 layers)	260.3	455.3	NR	NR	455.3	272.5	26.2	250
2 (12 layers)	330.4	733.6	179.8	217.3	516.3			
3 (12 layers)	321.9	695.7	179.5	216.4	479.2			
4 (12 layers)	265.2	472.2	NR	NR	472.2			
1 (16 layers)	332.5	742.5	153.9	159.1	583.5	288.8	31	286.1
2 (16 layers)	319.1	683.9	121.3	98.8	585			
3 (16 layers)	279.5	524.6	0.0[b]	0.0[b]	524.6			
4 (16 layers)	285.3	543.3	0.0[b]	0.0[b]	543.3			

NR = No reading (data point not valid)

[a] Partial penetration

[b] Ballistic limit velocity

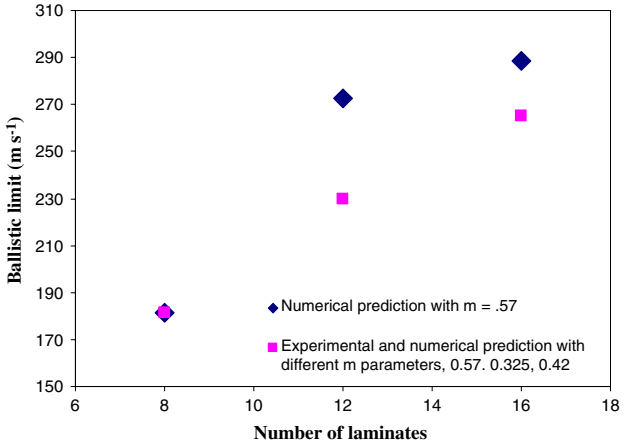

Fig. 4 Experimental results and numerical prediction of ballistic limit for the 8, 12, and 16 layer PP/E-glass laminates at different damage parameters, 0.57, 0.325, and 0.42

The Kinetic Energy (KE) plots with respect to time are shown in Fig. 5 for 8, 12, and 16 layer laminates using $m = 0.57$. Damage growth can be attributed to the combination of fiber failure modes including punch, shear plugging, fiber crush and tensile fiber failure. During the penetration process, a peak stress is generated in the contact region and propagates along the primary yarns which undergo tensile failure, while the secondary yarns undergo elastic deformation [23]. The steeper slope in projectile KE versus Time curves in Fig. 5 from approximately 0 to 0.01 ms is due to fiber crush which provides maximum resistance to penetration. The decrease in resistance to the penetration from approximately 0.01 to 0.03 ms is believed to be due to cone formation in the vicinity of the impact

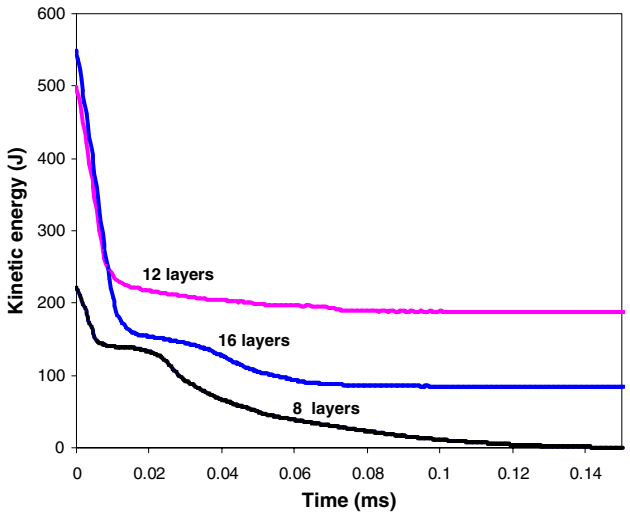

Fig. 5 Simulation results showing the kinetic energy lost by the projectile vs. time for the 8, 12, and 16 layer laminates at the experimentally predicted ballistic limit at damage parameter, $m = 0.57$

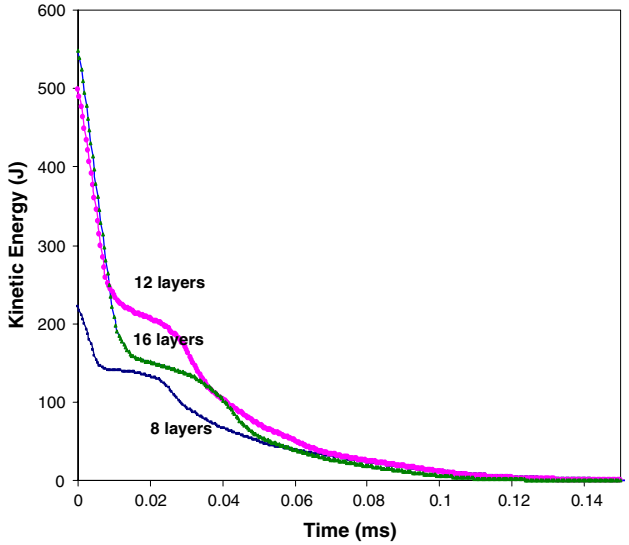

Fig. 6 Kinetic energy lost by the projectile vs. time for the 8, 12, and 16 layer laminates at ballistic limit at damage parameter, $m = 0.57$, 0.325 and 0.42, respectively

zone. This resulting deformation decreases the slope in the kinetic energy curve via kinetic energy transfer to the target. The increase in slope in the next time interval of 0.03–0.05 ms can be attributed to the bending stiffness of the laminate which offers resistance to the projectile penetration. At ballistic limit, the projectile comes to rest. The results of the kinetic energy versus time are more refined and in close agreement with the experiment for m values of 0.57, 0.325, and 0.42 for the 8, 12, and 16 layers, respectively, as shown in Fig. 6. It may be noted from the figure that the kinetic energy reaches zero at about the same time, i.e. 0.12 ms for 8, 12, and 16 layer laminates, respectively.

Discussion on damage parameter 'm'

With $m = 0.57$ energy absorption was under predicted for 12 and 16 layer laminates. This can be explained as follows. Because the number of elements through the thickness increases with increasing plate thickness, the bending stiffness of the plate increases. The simulations indicated that the laminates were stiffer (less energy absorption) in comparison to experimental results, Figs. 4 and 5. In order to increase the ductile response of the plates, the damage parameter m needed to be optimized. In order to confirm this assumption, a limited mesh sensitivity study was performed to describe the impact behavior of the 8 layer composite laminate. A fine mesh was developed using three elements per lamina, with dimensions, 0.175 x 0.175 x 0.225 mm^3 through the thickness, maintaining the thickness of each lamina constant. A 0.50 caliber right cylindrical steel projectile was used in the simulation to verify the experimentally determined ballistic limit

velocity of 181.3 m s^{-1}. Material parameters, contact and eroding damage parameters were kept the same as described above.

Figure 7a indicates that the projectile penetrated the E-glass/PP laminate with a residual velocity of 131.7 m s^{-1}, i.e. stiffer laminate response. The stiffer laminate response can be attributed to the higher number of elements through-the-thickness, which leads to higher global stiffness. Since each solid element is associated with a certain stiffness factor, it is expected that higher number of elements through-the-thickness will result in a stiffer material response. Hence, by optimizing the m parameter, the ductility (progressive damage) can be accounted for, as illustrated in Fig. 7b. For damage parameter $m = 0.03$, the projectile is arrested by the laminate at the ballistic limit. The time for perforation of the laminate was sensitive to the mesh size. The reduction in kinetic energy for the damage parameter $m = 0.57$ and 0.03 is illustrated in Fig. 8. It can be seen that the kinetic energy becomes zero in 0.17 ms for $m = 0.03$ (ballistic limit), while penetration occurs at 0.04 ms for $m = 0.57$. It may be noted that in the

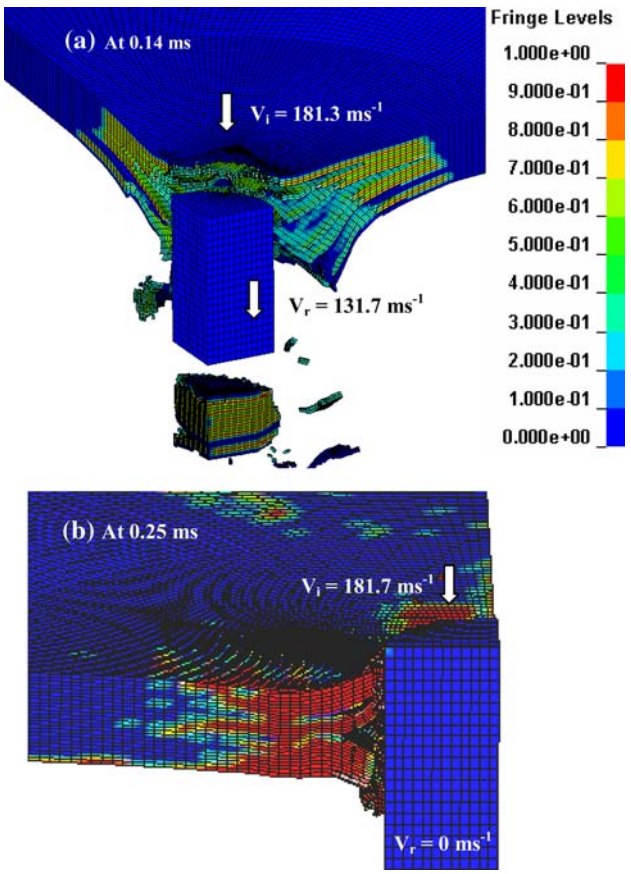

Fig. 7 (**a**) Simulated damage showing the projectile with an incident velocity of 181.3 ms^{-1} ripping through the 8 layer laminate with a residual velocity of 131.7 ms^{-1} at $m = 0.57$. (**b**) Projectile being arrested by the plate at experimentally observed ballistic limit at $m = 0.03$

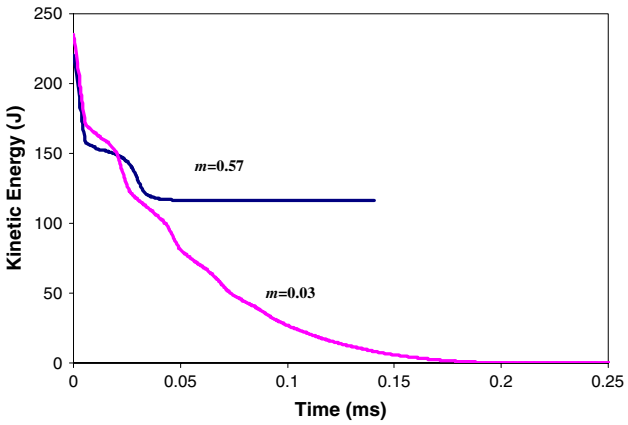

Fig. 8 Kinetic energy dissipation of the 0.50 caliber projectile impacted on fine meshed 8 layer plate at ballistic limit, 181.3 m s^{-1} at two different damage parameters, $m = 0.03$ and 0.57

present study the four strain softening (damage) parameters: m_1, m_2, m_3, and m_4 were assigned the same value in these simulations for the sake of simplicity, however, each parameter represents different damage mode, and hence should be assigned different values [27, 28]. This will be addressed in a future study.

Damage simulation and verification with experiment

Figure 9 compares the experimental and modeling results for transverse fiber failure in a 12-layer composite laminate (using history variable 7) for a 0.50 caliber projectile with a striking velocity of 330.4 m s^{-1}. As the laminate has a plain weave fabric architecture, fiber damage was found to propagate along primary yarns which were in the 0/90° direction. The secondary yarns underwent elastic deformation. The tensile fiber failure in a plain weave layer can be expressed by Eqs. 4 and 5 [33]:

$$f_{\text{fill}} = \left(\frac{\langle\sigma_1\rangle}{X_T}\right)^2 + \left(\frac{\tau_{12}^2 + \tau_{31}^2}{S_{XFS}^2}\right) - 1 = 0 \quad \text{if } \sigma_1 > 0 \tag{4}$$

$$f_{\text{warp}} = \left(\frac{\langle\sigma_2\rangle}{Y_T}\right)^2 + \left(\frac{\tau_{12}^2 + \tau_{23}^2}{S_{YFS}^2}\right) - 1 = 0 \quad \text{if } \sigma_2 > 0 \tag{5}$$

where X_T, Y_T, are the axial tensile strengths in the fill and warp directions, respectively, and S_{XFS}, S_{YFS} are the fiber shear strength. S_{YFS} can be expressed as [33]:

$$S_{YFS} = S_{XFS} * (X_T/Y_T) \tag{6}$$

Fiber shear strength and crush strength were chosen as 0.25 and 0.65 GPa, respectively, which were used to obtain the ballistic limit of 8 layers plate under normal incidence by a 0.30 caliber projectile impact.

In high strain rate loading, the material experiences higher stiffness because of strain rate sensitivity. The effect

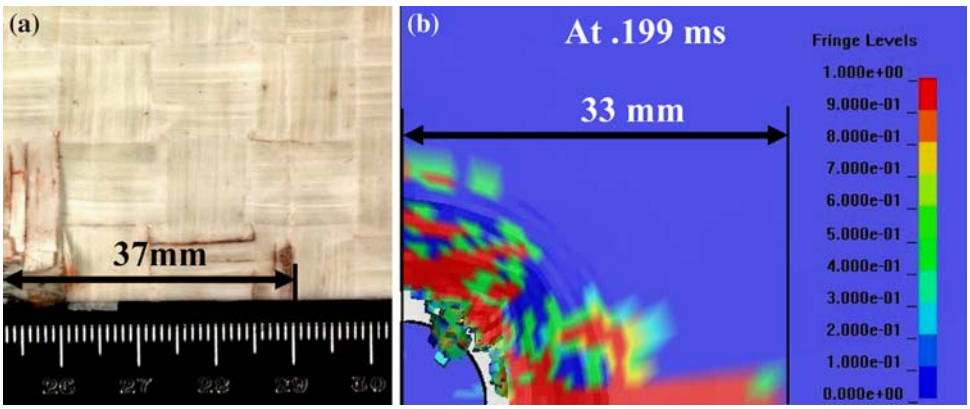

Fig. 9 Fiber failure along the primary yarns of 12 layer plate at $V_i = 330.4$ m s^{-1} (**a**) experimental and (**b**) simulation

of strain rate on the layer strength values can be expressed as [33]:

$$\{S_{\text{eff}}\} = \{S_0\}\left(1 + C_1 \ln \frac{\{\dot{\varepsilon}\}}{\dot{\varepsilon}_0}\right) \tag{7}$$

where S_{eff} is the effective strength at associated strain rate $\dot{\varepsilon}$, and S_0 is quasi-static strength at quasi static strain rate, $\dot{\varepsilon}_0$. A sensitivity analysis on the strain rate parameter, C_1, revealed values higher than the range 0.02–0.05 lead to numerical instability. A value of 0.025 was found reasonable while maintaining the energy balance. In MAT 162, the effect of strain rate on the elastic modulus of each lamina can be expressed as [33]:

$$E_{\text{eff}} = E_0\left[1 + (C_{\text{rate}}) \ln \frac{\{\dot{\varepsilon}\}}{\dot{\varepsilon}_0}\right] \tag{8}$$

where E_{eff} is the effective modulus at associated strain rate $\dot{\varepsilon}$, and E_0 is quasi-static modulus at quasi static strain rate, $\dot{\varepsilon}_0$. $C_{\text{rate}}(C_2,\ C_3,\ C_4)$ are the strain-rate constants. The values of C_2, C_3, and C_4 were taken from [27].

Delamination at the interface is one of the major failure mechanisms at the matrix mode, Fig. 10b. It is caused by the interlaminar stresses (σ_z, τ_{yz}, τ_{zx}) which initiate matrix microcracks which span the fiber-matrix interface and propagate along the fiber. MAT 162 provides an insight into the physics of the delamination of the composite plate as given by:

$$f_{\text{delamination}} = S_{\text{d}}\left(\frac{\langle\sigma_z\rangle}{Z_{\text{T}}}\right)^2 + \left(\frac{\tau_{yz}}{S_{yz}}\right)^2 + \left(\frac{\tau_{zx}}{S_{zx}}\right)^2 - 1 \tag{9}$$

where Z_{T}, S_{yz}, and S_{zx} are the failure strength properties and σ_z, τ_{yz}, and τ_{zx} are corresponding stress state. The delamination scale factor, S_{d} has a significant effect on ballistic limit velocity or energy absorption of composite plates. S_{d} is introduced to achieve better correlation with experimental values of delamination area by a scaling factor. The region (marked red, or shown as 35 mm on the scale) in Fig. 10 illustrates debonding of the fibers from the surrounding matrix and represents delamination failure of the

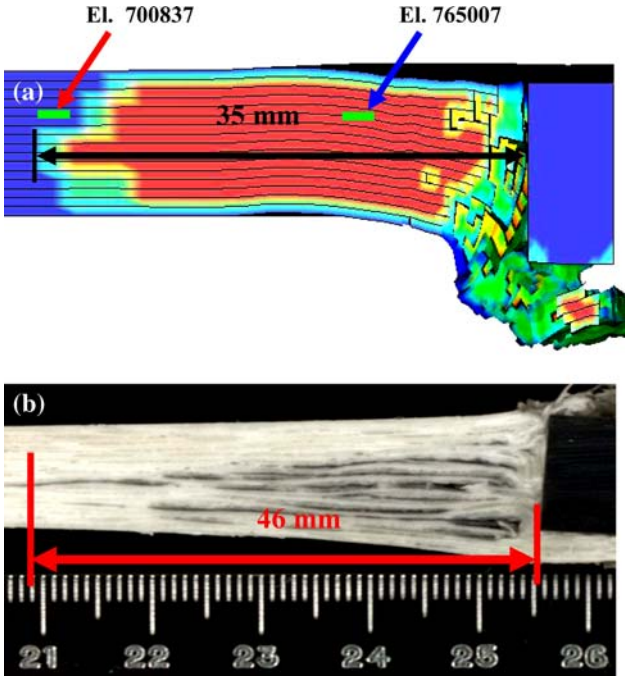

Fig. 10 Delaminated area of 16 layer composite at ballistic limit (**a**) simulation and (**b**) experimental (cross section)

laminates for both numerical and experimental observation for typical a 16-layer composite laminate at ballistic limit. The damage prediction was very close to the model prediction. Delamination factor, S_{d} was optimized iteratively and found to yield best results for a value of 0.3.

The interlaminar stress (σ_z, τ_{yz}, τ_{zx}) distribution for two representative elements (numbered 765007 and 700837) is shown in Fig. 11 (also refer to Fig. 10). Element 756007 is located in the delaminated region and the element 700837 is located in the region without delamination. Figure 11a shows that σ_z stress which is responsible for the opening mode (debonding) of the two surfaces was found to be maximum (70 MPa) for the element 765007 (delamination region) while the element 700837 (without delamination) experienced only 30 MPa along the z-direction. Delamination

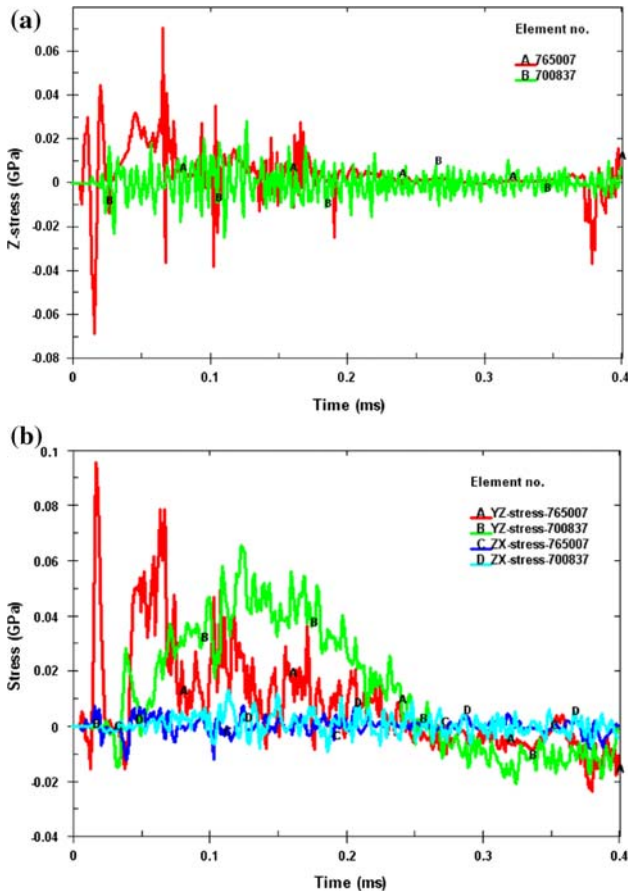

Fig. 11 Stress distributions vs. time in the elements 765007 and 700837 (**a**) σ_z stress (**b**) τ_{yz}, τ_{zx} stresses

propagates along the fiber-matrix interface due to the out of plane shear stresses (τ_{yz}, τ_{zx}). Figure 11b shows that τ_{zx} distribution at different stages is almost similar for the both elements. But element 765007 had undergone maximum τ_{yz} stress (95 MPa) at 0.025 ms while element 700837 witnesses a maximum of 68 MPa at 0.13 ms and starts decreasing thereafter.

Summary and conclusions

Progressive damage in E-glass/polypropylene composite laminate subjected to ballistic impact was investigated experimentally and from simulations. On the basis of the CDM technique, MAT 162 was implemented in LS-DYNA to observe the different damage modes in E-glass/PP thermoplastic composite laminate. The ballistic limit and energy absorption of the composite laminates were investigated using a 0.30 caliber right cylinder for a 8 layer laminate; and 0.50 caliber right cylinder projectiles for 8, 12, and 16 layer laminates, respectively. The numerical prediction of ballistic limit velocities of 8, 12 and 16-layer laminates agreed well with the experimental results; by incorporating the appropriate material softening parameter.

In the models examined, the damage parameter needed to be scaled up or down with respect to the laminate thickness (number of layers) and mesh size to obtain ballistic limit correlation to experiments. Similarly, the extent of delamination damage was very sensitive to the delamination factor S_d. For the present study, m values of 0.57, 0.325, and 0.42 were found to yield best correlation for the 8, 12, and 16 layer laminates, respectively; and a delamination factor S_d of 0.3. Material model MAT 162 could compute delamination at the interface areas where the surface elements failed as well as stress state in the vicinity of the delaminated region; thereby providing more efficient approach for modeling dynamic response of laminated composites.

Acknowledgement The support provided by Office of Naval Research (ONR) under Dr. Yapa Rajapakse, Project Manager is gratefully acknowledged.

References

1. Abrate S (1998) Impact on composite structures. Cambridge University Press, Cambridge, UK
2. Goldsmith W, Dharan CKH, Chang H (1995) Int J Impact Eng 32(1):89
3. Sun CT, Potti SV (1996) Int J Impact Eng 18(3):339. doi:10.1016/0734-743X(96)89053-1
4. Morye SS, Hine PJ, Duckett RA, Carr DJ, Ward IM (2000) Compos Sci Technol 60:2631. doi:10.1016/S0266-3538(00)00139-1
5. Department of Defense Test Method Standard V_{50} Ballistic Test for Armor, MIL-STD-662F, December 18, 1997
6. Mines RAW, Roach AM, Jones N (1999) Int J Impact Eng 22:561. doi:10.1016/S0734-743X(99)00019-6
7. Lee SWR, Sun CT (1993) Compos Sci Technol 49:369. doi:10.1016/0266-3538(93)90069-S
8. Zhu G, Goldsmith W, Dharan CKH (1992) Int J Solids Struct 29(4):399. doi:10.1016/0020-7683(92)90207-A
9. Zhu G, Goldsmith W, Dharan CKH (1992) Int J Solids Struct 29(4):421. doi:10.1016/0020-7683(92)90208-B
10. Okafor AC, Otieno AW, Dutta A, Rao VS (2001) Compos Struct 54:289. doi:10.1016/S0263-8223(01)00100-3
11. Wen HM (2000) Compos Struct 49:321. doi:10.1016/S0263-8223(00)00064-7
12. Wen HM (2001) Compos Sci Technol 61:1163. doi:10.1016/S0266-3538(01)00020-3
13. Abrate A (1994) Appl Mech Rev 47:517
14. Choi HY, Chang FK (1990) Impact damage threshold of laminated composite in failure criteria and analysis in dynamic response. AMD, 107, ASME Applied Mechanics Division, November, Dallas, TX, p 31
15. Davies GAO, Zhang X (1999) Int J Impact Eng 16:149. doi:10.1016/0734-743X(94)00039-Y
16. Richardson MOW, Wisheart MJ (1996) Composites 27(A):1123
17. Cantwell WJ, Morton J (1990) J Comp Sci Tech 38:119
18. Mahfuz H, Zhu Y, Haque A, Abutalib A, Vaidya U, Jeelani S, Gama B, Gillespie J, Fink B (2000) Int J Impact Eng. 24:203. doi:10.1016/S0734-743X(99)00047-0

19. DeLuca E, Prifti J, Betheney W, Chou SC (1998) J Comp Sci Tech 58:1453. doi:10.1016/S0266-3538(98)00029-3
20. Ladeveze P, LeDantec E (1992) Compos Sci Technol 43:257. doi:10.1016/0266-3538(92)90097-M
21. Allix O, Ladeveze P (1992) Compos Struct 22:235
22. Johnson AF, Pickett AK, Rozycki P (2001) J Comp Sci Tech 61:2183
23. Matzenmillar A, Lubliner J, Taylor RL (1995) Mech Mater 20:125
24. Williams KV, Vaziri R (2001) Comput Struct 79:997. doi:10.1016/S0045-7949(00)00200-5
25. Yen C-F (2002) Proceedings of the 7th international LS-DYNA users conference, Detroit, Michigan, p 15
26. Chan S, Fawaz Z, Behdinan K, Amid R (2007) Compos Struct 77:466. doi:10.1016/j.compstruct.2005.08.022
27. Brown K, Brooks R, Warrior N (2005) Proceedings of the 5th European LS-DYNA users conference, Birmingham, UK, May 25–26, 2005
28. Xiao JR, Gama BA, Gillespie JW (2007) Compos Struct 77:182. doi:10.1016/j.compstruct.2005.09.001
29. U.S. Department of Justice. Ballistic resistance of personal body armor. NIJ standard-0101.04, Office of Science and Technology, Washington, DC, June 2001
30. Altair HyperMesh. Altair Engineering, Inc.1820 E. Big Beaver Troy, MI, 1998
31. Engineering Technology Associates, Inc., Troy, MI, 2003
32. Livermore Software Technology Corporation, Livermore, 7374 Las Positas Road, CA, 2003
33. Hashin Z (1980) J Appl Mech 47:329
34. LS-DYNA Theoretical Manual, version 970. Livermore Software Tech. Corp., May 1998